Identification of peaks in multidimensional coincidence γ-ray spectra

Miroslav Morháč*, Ján Kliman,
Vladislav Matoušek, Martin Veselský and Ivan Turzo

Institute of Physics, Slovak Academy of Sciences,
Dúbravska cesta 9, 842 28 Bratislava,
Slovak Republic

Abstract

In the paper new algorithm to find peaks in two, three and multidimensional spectra measured in large multidetector γ-ray arrays are derived. Given the dimension m the algorithm is selective to m-fold coincidence peaks. It is insensitive to intersections of lower-fold coincidences, hereafter in the paper called ridges.

Keywords: Peak searching algorithm, Multidimensional peak identification, Smoothed second differences, Multidimensional gamma-ray spectra processing

PACS: 29.85.+c, 02.70.-c, 07.05.Kf

1 Introduction

The event data obtained with large γ-ray detector arrays such as EUROGAM [1], GAMMASPHERE [2], GASP[3] can be used to generate two, three, four or in general m-fold coincidence histograms, spectra. The progress in the nuclear structure understanding depends on the ability to analyze correctly these multidimensional spectra. Obviously the lack of methods of analyzing such data sets in powerful way can create a major obstacle to extract interesting physical information. The information contained in the many-fold coincidence spectra is overwhelming and so is difficulty of extracting all the detailed information contained in multidimensional peaks. The evaluation of multidimensional peaks starts with determination of their position in multidimensional space. Subsequently the peak searching procedure must recognize the shape of the found object and decide whether it is multidimensional Gaussian or not. Afterward the positions of identified peaks can be fed as initial estimates into peak fitting procedure for thorough analysis.

At present there exist several algorithms for automatic identification of peaks in one-dimensional spectra. One of the well-known peak searching algorithms is Mariscotti's method [4], which is based on evaluation of smoothed second differences. The modification of this method is presented in [5]. The basis of the methods presented in [6], [7], [8] is the smoothed first derivative that in the vicinity of peak changes the sign. Different approach based on Markov chains is used in peak searching method published in [9].

*E-mail: fyzimiro@savba.sk

Application of either of these methods cannot be directly extended to search for peaks in multidimensional space. In a simplified way one can think of one-dimensional spectrum as a composition of background, peaks and statistical disturbances (noise). However in multidimensional γ-ray spectra things are completely different. For instance two-dimensional γ-ray spectrum, without considering noise, contain continuous background, one-fold coincidences (ridges as a result of coincidences peak-background) in both directions and two-fold coincidence γ-ray peaks. We are interested only in and looking for two-fold coincidence peaks. The proposed algorithm must be insensitive to the intersections of one-fold coincidence ridges that at the first glance look like two-dimensional peaks. The method must be able to distinguish between intersection of two ridges and two-fold coincidence peak. The situation is more complicated by the fact that two-dimensional peaks are usually located at the points of ridges crossing.

Analogously three-dimensional spectra contain continuous background, one-fold and two-fold coincidences (ridges), in all three directions, and three-fold coincidence peaks. Again we are interested only in identification of three-fold coincidence peaks. The algorithm should ignore the intersections of either one-fold or two-fold coincidence ridges. In general in m-dimensional γ-ray spectra the algorithm should identify only m-fold coincidence peaks.

The aim of the paper is to propose an algorithm for identification of 2, 3, ... m-fold coincidence peaks in 2, 3, ..., m-dimensional γ-ray spectra.

2 Peak searching algorithm in two-dimensional spectra

We suppose that the number of counts in a two-dimensional γ-ray spectrum in the channel x, y can be approximated by

$$N(x,y) = G_1(x,y) + G_2(x) + G_3(y) + B + Cx + Dy \tag{1}$$

The two-dimensional Gaussian is defined as

$$G_1(x,y) = A_1 \exp\left\{-\frac{1}{2(1-\rho^2)}\left[\frac{(x-x_1)^2}{\sigma_{x_1}^2} - \frac{2\rho(x-x_1)(y-y_1)}{\sigma_{x_1}\sigma_{y_1}} + \frac{(y-y_1)^2}{\sigma_{y_1}^2}\right]\right\} \tag{2}$$

where x_1, y_1 is its position, σ_{x_1} and σ_{y_1} are standard deviations of normal distribution in the directions x and y, respectively and ρ is correlation coefficient. Analogously one-dimensional ridges parallel with axes y and x, can be described by

$$G_2(x) = A_2 \exp\left\{-\frac{(x-x_2)^2}{2\sigma_{x_2}^2}\right\} \tag{3}$$

and

$$G_3(y) = A_3 \exp\left\{-\frac{(y-y_3)^2}{2\sigma_{y_3}^2}\right\} \tag{4}$$

respectively. Within short interval we assume that the background in (1) can be approximated by linear function

$$B + Cx + Dy. \tag{5}$$

Obviously the mixed partial second derivative of (1) in both dimensions $\frac{\partial^4 N(x,y)}{\partial x^2 \partial y^2}$ does not depend on $G_2(x), G_3(y)$ and linear background.

Because of discrete nature of channel counts we shall replace the mixed partial second derivatives by the mixed partial second differences in both dimensions

$$\begin{aligned} S(i,j) &= N(i+1,j+1) - 2N(i,j+1) + N(i-1,j+1) \\ &\quad -2N(i+1,j) + 4N(i,j) - 2N(i-1,j) \\ &\quad +N(i+1,j-1) - 2N(i,j-1) + N(i-1,j-1) \end{aligned} \tag{6}$$

In order to eliminate statistical fluctuations we shall employ the smoothed mixed partial second differences in both dimensions.

The smoothing is achieved by summing $S(i,j)$ in a given window

$$S_w(i,j) = \sum_{i_1=i-r}^{i+r} \sum_{j_1=j-r}^{j+r} S(i_1,j_1) \tag{7}$$

where the window $w = 2r+1$. In accordance with [4] the repetitive application of (3) yields the general smoothed mixed partial second differences in both dimensions, $S_{z,w}(i,j)$, where z is the number of repetitions. For the sake of simplicity, from now on in the paper, we shall call the difference spectrum $S_{z,w}(i,j)$ as the two-parameter smoothed second differences or two-parameter SSD.

Then the contents of the channel i,j of this difference spectrum can be expressed

$$S_{z,w}(i,j) = \sum_{i_1=i-r}^{i+r} \sum_{j_1=j-r}^{j+r} C_{z,w}(i_1-i, j_1-j) N(i_1,j_1) \tag{8}$$

where $r = z \cdot m + 1, m = (w-1)/2$. From (6) and (7) it implies that the elements of the filter matrix $C_{z,w}(i,j)$ can be factorized to products of vector elements

$$C_{z,w}(i,j) = C_{z,w}(i) \cdot C_{z,w}(j) \tag{9}$$

The vector elements $C_{z,w}(i), i \in < -r, r >$, can be calculated using recursive formula

$$C_{z,w}(i) = \sum_{i_1=i-r}^{i+r} C_{z-1,w}(i_1) \tag{10}$$

where $i \in < -z \cdot r - 1, z \cdot r + 1 >$ and

$$C_{0,w} = \begin{cases} -2 & \text{if } i = 0 \\ 1 & \text{if } |i| = 1 \\ 0 & \text{otherwise.} \end{cases}$$

In analogy with the algorithm in [4] and regarding to (9), we define standard deviation of two-parameter SSD

$$F_{z,w}(i,j) = \sqrt{\sum_{i_1=i-r}^{i+r} \sum_{j_1=j-r}^{j+r} C^2_{z,w}(i_1-i) C^2_{z,w}(j_1-j) N(i_1,j_1)} \tag{11}$$

Another way to compute the coefficients of the filter vector C is used [5]. The vector C is defined as the second derivative of the Gaussian

$$C_\sigma(i) = \frac{d^2}{dx^2} \exp\left(-\frac{x^2}{2\sigma^2}\right) \Bigg|_{\, x = i} \tag{12}$$

where σ is standard deviation of searched peaks. The replacement of the filter coefficients $C(i)$ from (12) into (8), (9), (11) is straightforward. The choice of the method employed in peak searching procedure is optional and depends on application. While in the first case the free parameters are z, w, in the second method the only free parameter is σ. In general independently of the way of calculation of the SSD filter the relations (8), (11) can be expressed

$$S(i,j) = \sum_{i_1=i-r}^{i+r} \sum_{j_1=j-r}^{j+r} C(i_1-1)C(j_1-j)N(i_1,j_1) \tag{13}$$

$$F(i,j) = \sqrt{\sum_{i_1=i-r}^{i+r} \sum_{j_1=j-r}^{j+r} C^2(i_1-i)C^2(j_1-j)N(i_1,j_1)} \tag{14}$$

Two-parameter SSD spectrum calculated using above presented algorithm is insensitive to intersection of two ridges representing coincidence peak - background. For illustration purpose, using (1), (2), (3), (4), (5) we have generated (synthetic) spectrum (Fig. 1) with two two-dimensional Gaussians

$$\begin{aligned} &G_{1A}(A_{1A}=100, \quad x_{1A}=60, \quad y_{1A}=8), \\ &G_{1B}(A_{1B}=50, \quad x_{1B}=180, \quad y_{1B}=200) \end{aligned} \tag{15}$$

two ridges parallel with y axis

$$\begin{aligned} &G_{2A}(A_{2A}=200, \quad x_{2A}=60) \\ &G_{2B}(A_{2B}=180, \quad x_{2B}=180) \end{aligned} \tag{16}$$

two ridges parallel with x axis

$$\begin{aligned} &G_{3A}(A_{3A}=200, \quad x_{3A}=80), \\ &G_{3B}(A_{3B}=500, \quad x_{3B}=200) \end{aligned} \tag{17}$$

and linear background

$$800 - 1,176.x - 1,96.y$$

Parameters σ were set to 6 and $\rho = 0$. At the first glance it is very difficult to estimate positions of two-dimensional Gaussians. Their positions are in Fig. 1 denoted by points A, B. The difference spectrum calculated according to (8), (9), (10) with $w = 7, z = 7$ is shown in Fig. 2. Apparently the difference spectrum reflects only the presence of two-dimensional peaks G_{1A}, G_{1B}. It ignores linear background, ridges $G_{2A}, G_{2B}, G_{3A}, G_{3B}$ and their intersections.

Now let us have a closer look at the shape of the difference spectrum of the two-dimensional peak (Fig. 3). We can observe that in the slices A, B, C, D the courses of the curves correspond to the smoothed second difference spectrum of one-dimensional Gaussian. In the slices E, F they correspond to negation of the smoothed second difference spectrum of one-dimensional Gaussian. The difference spectrum and its standard deviation for one-dimensional Gaussian are given in Fig. 4 According to Fig. 4 to decide whether a found object is Gaussian peak or not we need to define points $i_1 - i_6$. Subsequently we can apply evaluation criteria for one-dimensional Gaussian described in detail in [4]. We repeat this procedure for each dimension (in our example slices E, F).

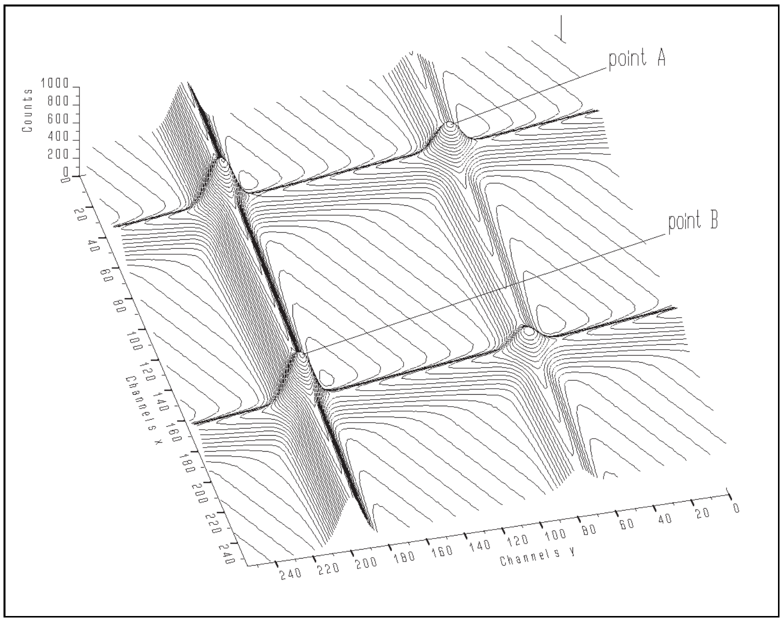

Figure 1: Synthetic spectrum with two two-dimensional Gaussians located at the points A, B

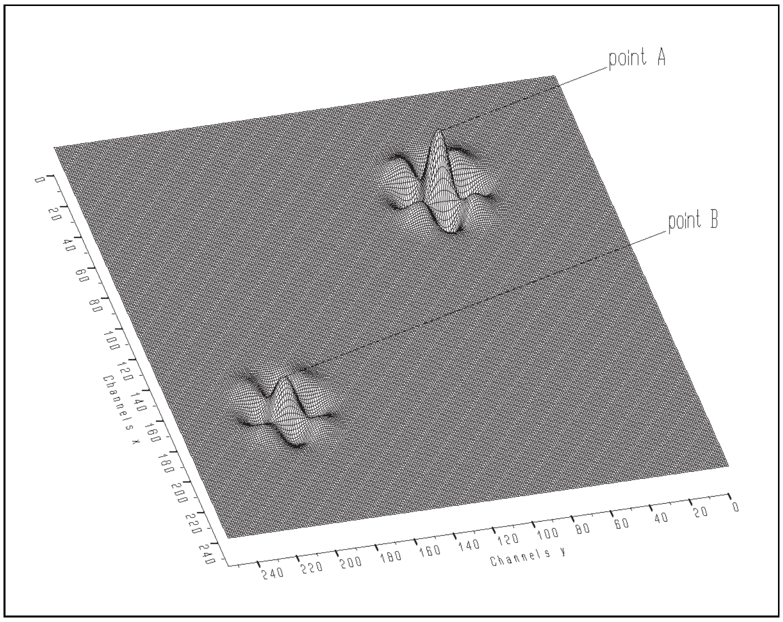

Figure 2: The difference spectrum for the spectrum from Fig. 1

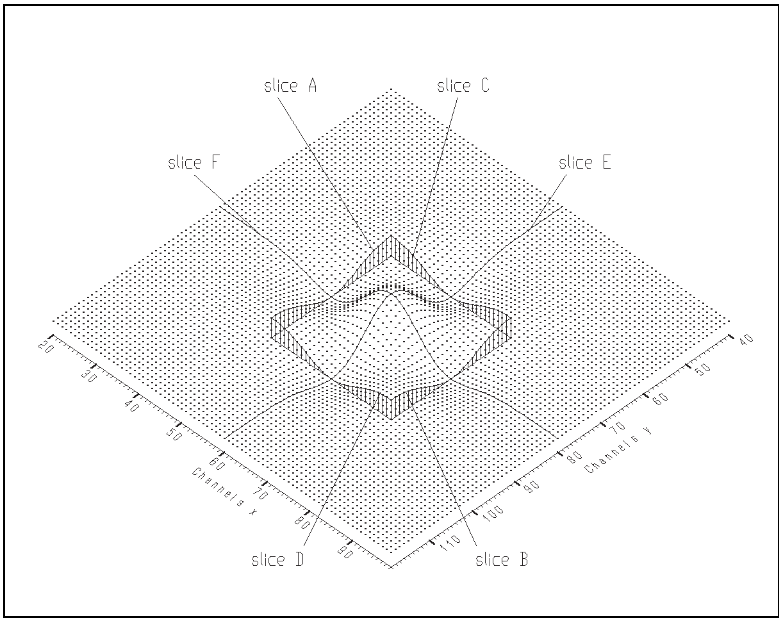

Figure 3: The shape of the difference spectrum of the two-dimensional Gaussian

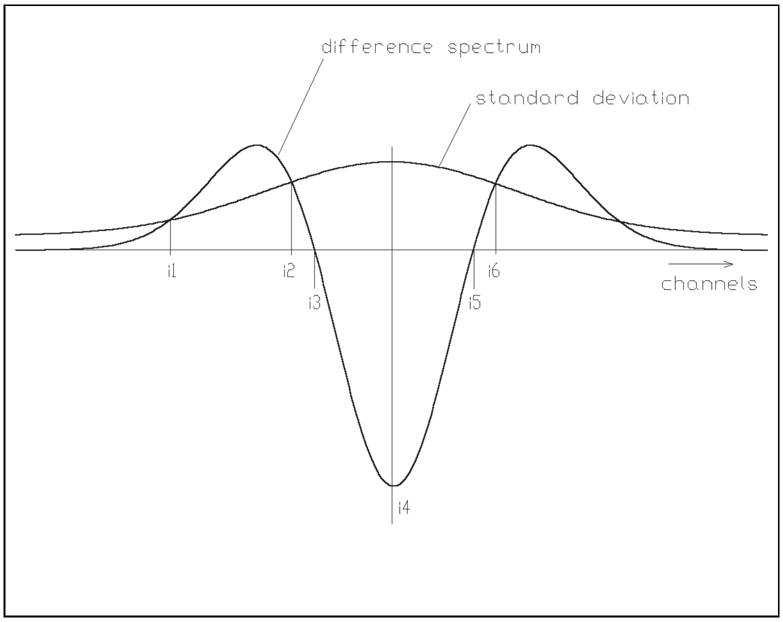

Figure 4: The difference spectrum and its standard deviation for one-dimensional Gaussian

When looking at Figs. 2, 3 more thoroughly we can observe that one two-dimensional peak gives rise to 5 local maxima in the difference spectrum. The position of one of the local maxima located in the middle of the surrounding ones corresponds to the position of two-dimensional peak. Let us call this local maximum as true and the remaining four local maxima as false (Fig. 5) Once we have calculated two-parameter SSD (difference spectrum) the problem is how

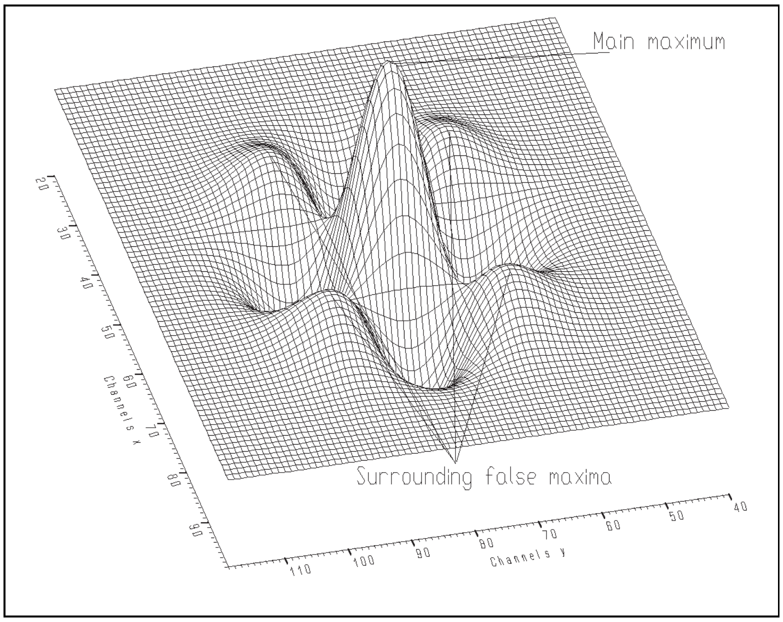

Figure 5: True and false local maxima for the two-dimensional peak

to distinguish between true and false maxima. False maxima should be ignored by the searching algorithm. In simple instances, when we have just few peaks in the spectrum it can seem trivial. It can be solved by finding groups of corresponding five maxima. Such an example can be illustrated by the spectrum with one peak from experiment of positron annihilation (Fig. 6) [10]. Its two-parameter SSD is shown in Fig. 7. However when having large number of peaks in evaluated spectrum, which is usually the case of γ-ray spectra, this task is very difficult. Figs. 8 and 9 give an example of such a two-dimensional γ-ray spectrum and its two-parameter SSD, respectively. From Fig. 9 it is obvious that it is practically impossible to find groups of corresponding five local maxima. The true and false local maxima of two-parameter SSD of neighbouring peaks in original spectrum can either be mixed or can mutually coincide. Therefore it is needed to suppress in a way the false maxima in the two-parameter SSD.

In keeping with (7), (8), (13) we shall define spectra of the one-parameter smoothed second derivatives (one-parameter SSD) in both x and y independent variables,

$$X(i,j) = \sum_{i_1=i-r}^{i+r} C(i_1 - i)N(i_1, j) \tag{18}$$

and

$$Y(i,j) = \sum_{j_1=j-r}^{j+r} C(j_1 - j)N(i, j_1) \tag{19}$$

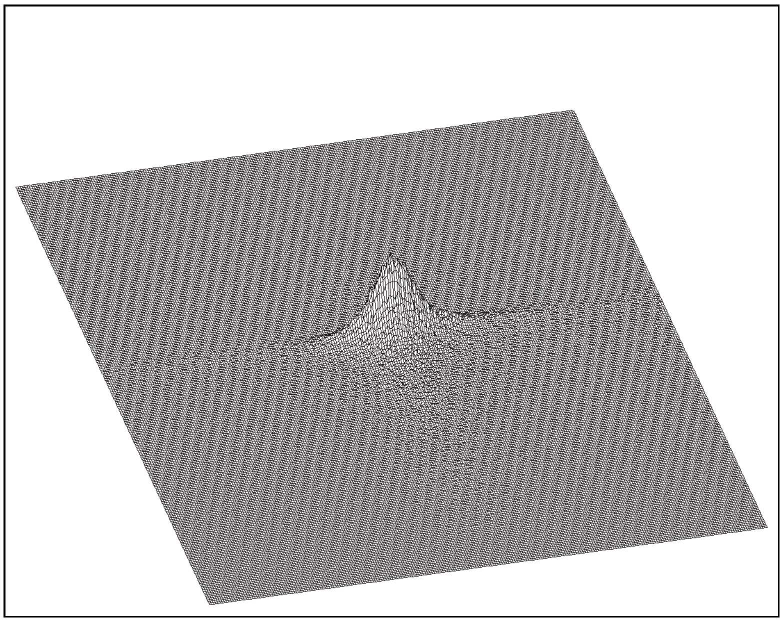

Figure 6: Spectrum with one peak from experiment of positron annihilation

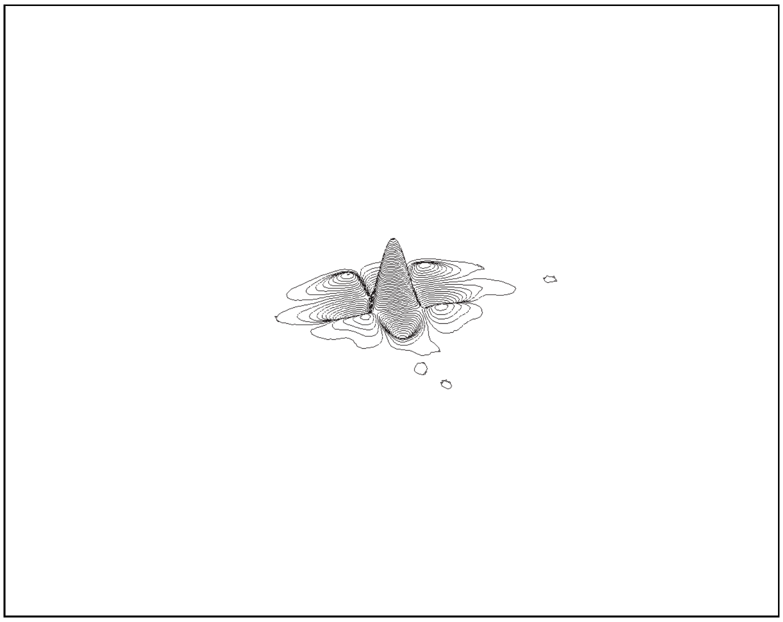

Figure 7: Two-parameter SSD spectrum from Fig. 6

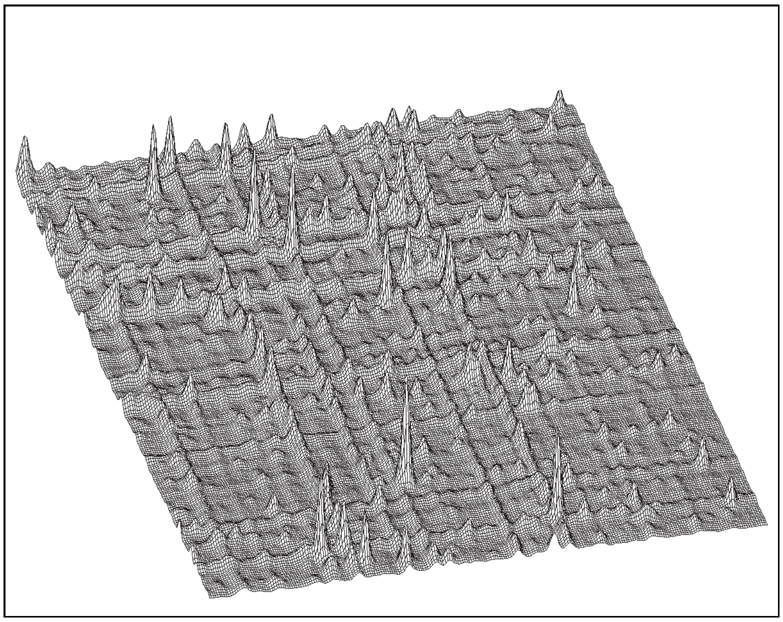

Figure 8: Two-dimensional γ-ray spectrum

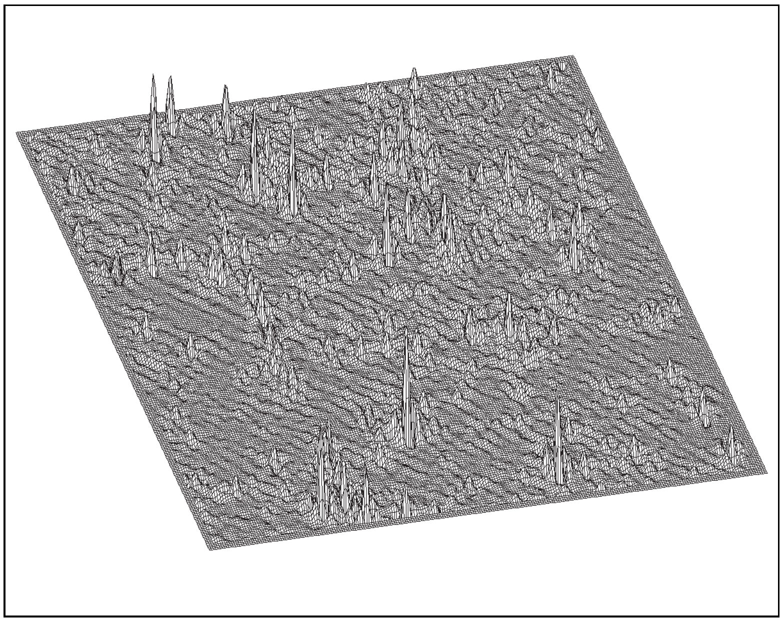

Figure 9: Two-parameter SSD spectrum from Fig. 8

	$C_s(i,j)$			$C_x(i,j)$			$C_y(i,j)$		
j_1 \ i_1	$i-1$	i	$i+1$	$i-1$	i	$i+1$	$i-1$	i	$i+1$
$j-1$	1	-2	1	1	-2	1	1	1	1
j	-2	4	-2	1	-2	1	-2	-2	-2
$j+1$	1	-2	1	1	-2	1	1	1	1

Table 1: Examples of the filters $C_s(i,j)$ for $z = w = 0$ according to (10) for two-parameter SSD and $C_x(i), C_y(j)$ for one-parameter SSDs in two-dimensional space.

where the coefficients of the filter C are defined either according to (10) or (12).

As a step toward understanding the difference among filters in the Table 1 we give an example of the filter $C_s(i,j)$ for $z = w = 0$ according to (10) for two-parameter SSD as well as examples of filters $C_x(i), C_y(j)$ for one-parameter SSDs in two-dimensional space.

From the filters defined in this way we can observe that in the expected position of two-dimensional peak $i_1 = i, j_1 = j$ it holds

$$\begin{aligned} C_s(i,j) &> 0 \\ C_x(i) &< 0 \\ C_y(j) &< 0 \end{aligned}$$

Likewise from the definitions of two-parameter SSD given by (7), (8), (9), (10), (13) and one-parameter SSD given by (18), (19) as well as from the Fig. 4 and presented examples it is apparent that in the position of true local maximum of two-parameter SSD (i_t, j_t) the following condition is satisfied

$$S(i_t, j_t) > 0 \quad \text{and} \quad X(i_t, j_t) < 0 \quad \text{and} \quad Y(i_t, j_t) < 0. \tag{20}$$

Along with this condition also the following conditions, saying that in the point (i_t, j_t) one-parameter SSDs in both dimensions have local minima, must be satisfied

$$X(i_{t-1}, j_t) \geq X(i_t, j_t) \leq X(i_{t+1}, j_t) < 0. \tag{21}$$

$$Y(i_t, j_{t-1}) \geq Y(i_t, j_t) \leq Y(i_t, j_{t+1}) < 0. \tag{22}$$

The condition (20) is not satisfied in the point of false local maxima in two-parameter SSD (i_f, j_f), i.e.,

$$S(i_f, j_f) > 0 \quad \text{and} \quad \Big(X(i_f, j_f) \geq 0 \quad \text{or} \quad Y(i_f, j_f) \geq 0\Big). \tag{23}$$

By application of the condition (20) we can unambiguously distinguish between true and false maxima in two-parameter SSD. The example of two-parameter SSD spectra from Figs. 7, 9 after application of the condition (20) are presented in Figs. 10, 11. Summarizing all together

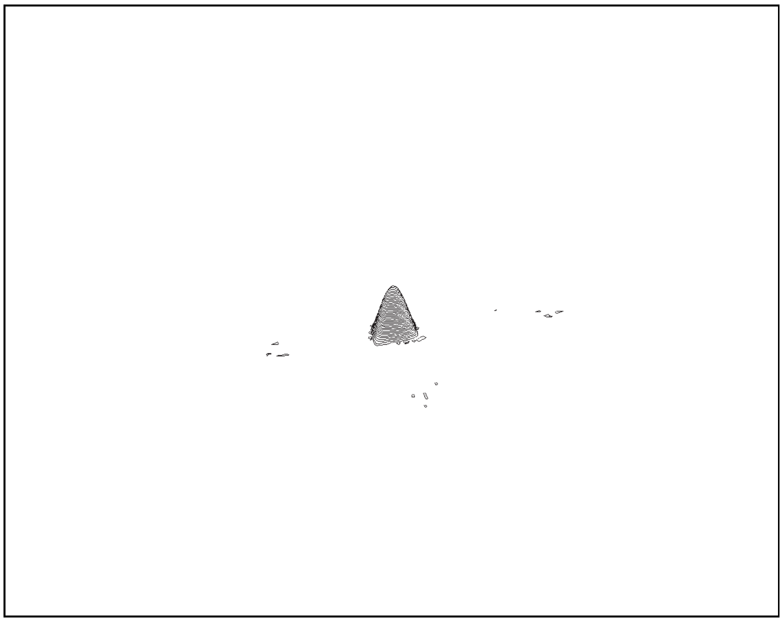

Figure 10: Two-parameter SSD spectrum from Fig. 7 after application of the condition (20)

the algorithm to search for peaks in two-dimensional spectrum is as follows:

a. using (13) we calculate spectrum of the smoothed second differences in both dimensions (two-parameter SSD) $S(i, j)$

b. using (14) we calculate spectrum of standard deviation of the smoothed second differences in both dimensions $F(i, j)$.

c. for $i \in < 0, n_1 - 1 >, j \in < 0, n_2 - 1 >$, where n_1, n_2 are sizes of the spectrum, we search for local maxima in the spectrum of two-parameter SSD - $S(i, j)$.

d. once we have found a local maximum in the position i_l, j_l then using (18) and (19) we calculate spectra of one-parameter SSD $X(i_l, j_l)$ and $Y(i_l, j_l)$ respectively. Then applying condition (20) we decide whether the found local maximum is true or false.

e. if the condition (20) is satisfied we test the slice $S(i, j_l), F(i, j_l), i \in < 0, n_1 - 1 >$ (slice F in Fig. 3) by Mariscotti's criteria for the shape of the peak in x dimension. Likewise we test the slice $S(i_j, j), F(i_l, j), j \in < 0, n_2 - 1 >$ (slice E in Fig. 3) by the same criteria for the shape of the peak in y dimension.

f. if the shape of the peak in both dimensions satisfies these criteria we have found two-dimensional peak in the position i_l, j_l.

g. we repeat the whole procedure for another local maximum from the point c on.

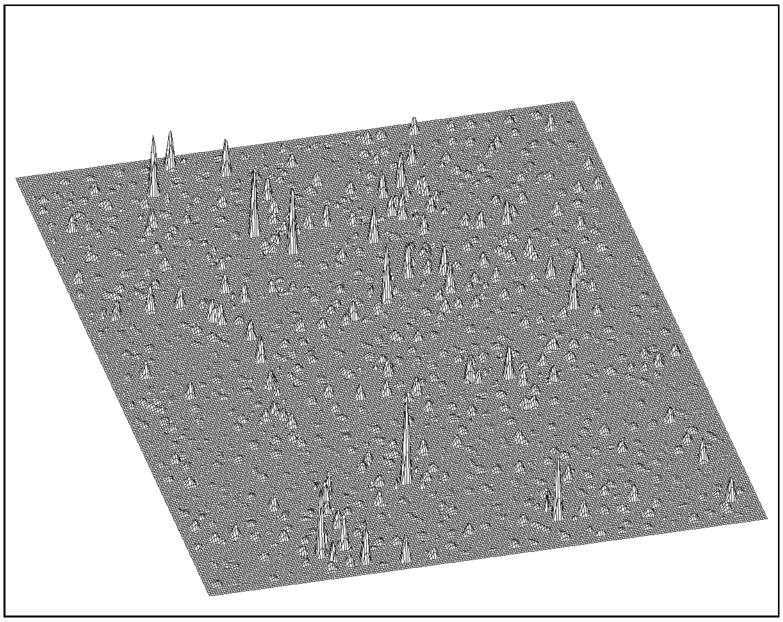

Figure 11: Two-parameter SSD spectrum from Fig. 9 after application of the condition (20)

3 Peak searching algorithm for three and m-dimensional spectra.

The algorithm of peak searching in two-dimensional spectra described so far can be generalized to three-, four- and m-dimensional spectra. Analogously to two-dimensional case for three-dimensional spectrum we can define spectrum of the smoothed second differences in all three dimensions, three-parameter SSD,

$$S(i,j,k) = \sum_{i_1=i-r}^{i+r} \sum_{j_1=j-r}^{j+r} \sum_{k_1=k-r}^{k+r} C(i_1-i, j_1-j, k_1-k) N(i_1, j_1, k_1) \tag{24}$$

and its standard deviation

$$F(i,j,k) = \sqrt{\sum_{i_1=i-r}^{i+r} \sum_{j_1=j-r}^{j+r} \sum_{k_1=k-r}^{k+r} C^2(i_1-i, j_1-j, k_1-k) N(i_1, j_1, k_1)}. \tag{25}$$

If we choose the filter according to (10), we obtain

$$C_s(i,j,k) = C(i)C(j)C(k) \tag{26}$$

With a view to explaining some facts in the Table 2 we present this three-dimensional filter for $z = w = 0$.

With regard to (10) from the Table 2 we can see that in the point of expected position of three-dimensional peak $i_1 = i, j_1 = j, k_1 = k$.

$$C_s(i,j,k) < 0 \tag{27}$$

	$k_1 = k-1$			$k_1 = k$			$k_1 = k+1$		
i_1 / j_1	$i-1$	i	$i+1$	$i-1$	i	$i+1$	$i-1$	i	$i+1$
$j-1$	1	-2	1	-2	4	-2	1	-2	1
j	-2	4	-2	4	-8	4	-2	4	-2
$j+1$	1	-2	1	-2	4	-2	1	-2	1

Table 2: An example three-dimensional filter for $z = w = 0$

and

$$C(i) < 0, \qquad C(j) < 0, \qquad C(k) < 0 \tag{28}$$

Obviously the point $i_1 = i, j_1 = j, k_1 = k$ is the only point in the Table 2 that satisfies the conditions (27) and (28). Further analogously to (18), (19) we define spectra of the one-parameter smoothed second differences in all three dimensions

$$X(i,j,k) = \sum_{i_1=i-r}^{i+r} C(i_1 - i)N(i_1, j, k), \tag{29}$$

$$Y(i,j,k) = \sum_{j_1=j-r}^{j+r} C(j_1 - j)N(i, j_1, k), \tag{30}$$

$$Z(i,j,k) = \sum_{k_1=k-r}^{k+r} C(k_1 - k)N(i, j, k_1). \tag{31}$$

The spectrum of three-parameter SSD defined according to (24) is insensitive to continuous background, one-fold coincidences peak-background, two-fold coincidences peak-background or to any combinations of their intersections. Now in the position of expected three-dimensional peak the function $S(i,j,k)$ has corresponding local minimum. Besides in the vicinity of three-dimensional peak the function $S(i,j,k)$ contains additional 12 local minima. Again the true local minimum must be distinguished from the false local minima. Analogously with the condition (20) and in line with above given example of the filter C one can conclude that in the position of true local minimum (i_t, j_t, k_t) it holds

$$\begin{array}{llll} S(i_t,j_t,k_t) < 0 & \text{and} & X(i_t,j_t,k_t) < 0 & \text{and} \\ Y(i_t,j_t,k_t) < 0 & \text{and} & Z(i_t,j_t,k_t) < 0 & \end{array} \tag{32}$$

Now we can generalize the searching algorithm for m-dimensional spectra. For the spectrum of m-parameter SSD we can write

$$\begin{aligned} S \quad & (i_1, i_2, \ldots, i_m) = \\ = \quad & \sum_{a_1=i_1-r}^{i_1+r} \sum_{a_2=i_2-r}^{i_2+r} \cdots \sum_{a_m=i_m-r}^{i_m+r} C(a_1 - i_1, a_2 - i_2, \ldots, a_m - i_m) N(a_1, a_2, \ldots, a_m). \end{aligned} \tag{33}$$

Its standard deviation is

$$\begin{aligned} F \quad & (i_1, i_2, \ldots, i_m) = \\ = \quad & \sqrt{\sum_{a_1=i_1-r}^{i_1+r} \sum_{a_2=i_2-r}^{i_2+r} \cdots \sum_{a_m=i_m-r}^{i_m+r} C^2(a_1 - i_1, a_2 - i_2, \ldots, a_m - i_m) N(a_1, a_2, \ldots, a_m)}. \end{aligned} \tag{34}$$

Similarly the spectra of one-parameter SSD are

$$\begin{aligned} X_1(i_1, i_2, \ldots, i_m) &= \sum_{a_1=i_1-r}^{i_1+r} C(a_1 - i_1) N(a_1, i_2, \ldots, i_m) \\ X_2(i_1, i_2, \ldots, i_m) &= \sum_{a_2=i_2-r}^{i_2+r} C(a_2 - i_2) N(i_1, a_2, \ldots, i_m) \\ &\vdots \\ X_m(i_1, i_2, \ldots, i_m) &= \sum_{a_m=i_m-r}^{i_m+r} C(a_m - i_m) N(i_1, i_2, \ldots, a_m) \end{aligned} \tag{35}$$

Provided we have defined the filter C either according to (9), (10), or to (12) then in the position of m-dimensional peak $(i_1, i_2, \ldots, i_m)$ one can conclude

$$\begin{aligned} &\text{a. if } m \text{ is odd} \quad S(i_1, i_2, \ldots, i_m) < 0 \\ &\text{b. if } m \text{ is even} \quad S(i_1, i_2, \ldots, i_m) > 0 \end{aligned} \tag{36}$$

Spectrum of m-parameter SSD (33) is insensitive to lower-fold coincidences of peak-background. It is selective only to m-fold coincidence peaks. However around the m-dimensional peak it generates false local extremes, if m is odd - minima, if m is even - maxima. Their number is

a. if m is odd
$$\frac{3^m - 1}{2} - 1$$

b. if m is even
$$\frac{3^m - 1}{2}.$$

In analogy to two- and three-dimensional spectra the false local extremes can be suppressed by applying conditions

$$X_j(i_1, i_2, \ldots, i_m) < 0; \qquad j \in < 1, m > \tag{37}$$

where $X_j(i_1, i_2, \ldots, i_m)$ are calculated according to (35).

Finally in general case for m-dimensional spectra the searching algorithm of m-fold coincidence peaks can be expressed as follows :

a. using (33) we calculate spectrum of the smoothed second differences in all dimensions (m-parameter SSD) $S(i_1, i_2, \ldots, i_m)$.

b. using (34) we calculate spectrum of standard deviation of the smoothed second differences in all dimensions $F(i_1, i_2, \ldots, i_m)$.

c. for $i_j \in < 0, n_{j-1} >, j \in < 1, m >$, where $n_1, n_2, \ldots, n_m$ are sizes of the spectrum, we search for local extremes

   1. if m is odd - local minima
   2. if m is even - local maxima

   in $S(i_1, i_2, \ldots, i_m)$.

d. once we have found an appropriate local extreme in the point $l_1, l_2, \ldots, l_m$ then using (35) we calculate spectra of 1-parameter SSD

$$X_1(l_1, l_2, \ldots, l_m), \ldots, X_m(l_1, l_2, \ldots, l_m).$$

   Then applying conditions (37) we decide whether the found local extreme is true or false.

e. if the conditions (37) are satisfied we test the slices

$$\begin{array}{llll} (-1)^{m+1} & S(i_1, l_2, \ldots, l_m), & F(i_1, l_2, \ldots, l_m), & i_1 \in < 0, n_1 > \\ (-1)^{m+1} & S(l_1, i_2, \ldots, l_m), & F(l_1, i_2, \ldots, l_m), & i_2 \in < 0, n_2 > \\ \vdots & & & \\ (-1)^{m+1} & S(l_1, l_2, \ldots, i_m), & F(l_1, l_2, \ldots, i_m), & i_m \in < 0, n_m > \end{array}$$

   by Mariscotti's criteria for the shape of the peak in each dimension.

f. if the shape of the peak in all dimensions satisfies these criteria we have found m-dimensional peak in the position $(l_1, l_2, \ldots, l_m)$

g. we repeat the whole procedure for another local extreme from the point c on.

4 Results

The algorithms to search for peaks in the coincidence two-, three-dimensional spectra described so far have been tested using computer generated synthetic spectra. Using this kind of spectra we know beforehand the result that should be obtained and thus we can verify the reliability of the algorithms. In Fig. 12 we can see example of such a two-dimensional spectrum. It contains two- dimensional peaks, ridges in both dimensions and noise. The peak searching procedure

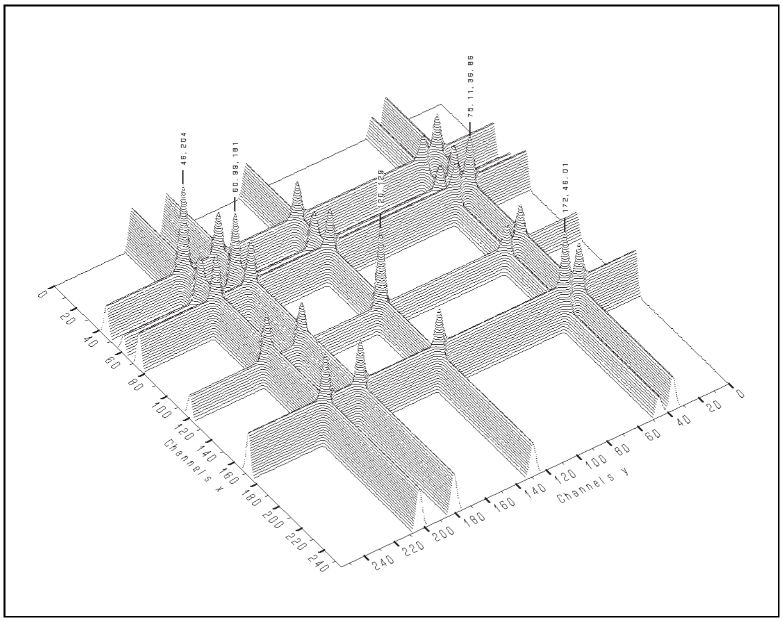

Figure 12: Synthetic two-dimensional spectrum with found peaks denoted by markers

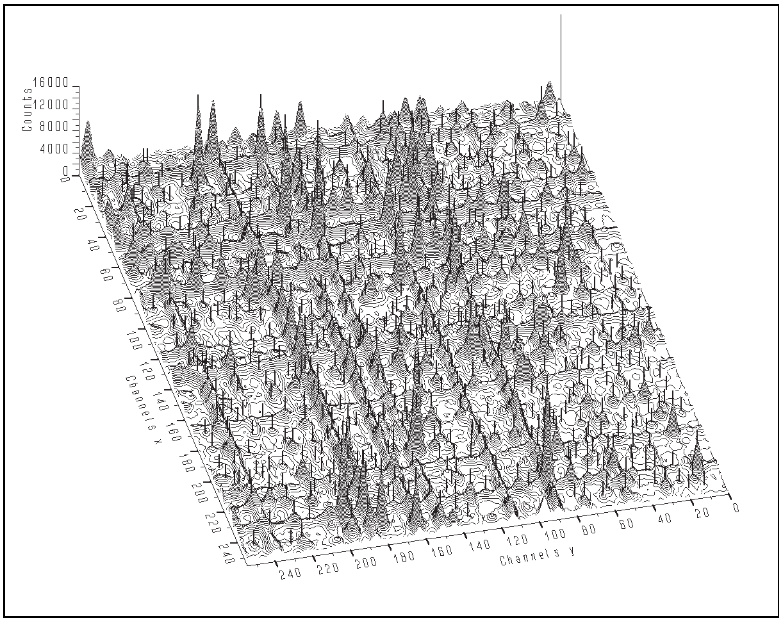

Figure 13: Coincidence two-dimensional γ-ray spectrum with found peaks

finds two-dimensional peaks exactly at the location where they were generated. The markers denote the positions of found two-dimensional peaks. The method is insensitive to the crossing of ridges. Fig. 13 illustrates real coincidence two-dimensional γ-ray spectrum. Again found two-dimensional peaks are denoted by markers. Similarly we have tested the peak searching algorithm for three-dimensional spectra. In Fig. 14 we can see again the synthetic three-dimensional spectrum. The channels are represented by balls. Their sizes are proportional to the counts the channels contain. The spectrum is composed of three-dimensional peaks, ridges of one and two-fold coincidences and noise. Again the peak searching procedure determines

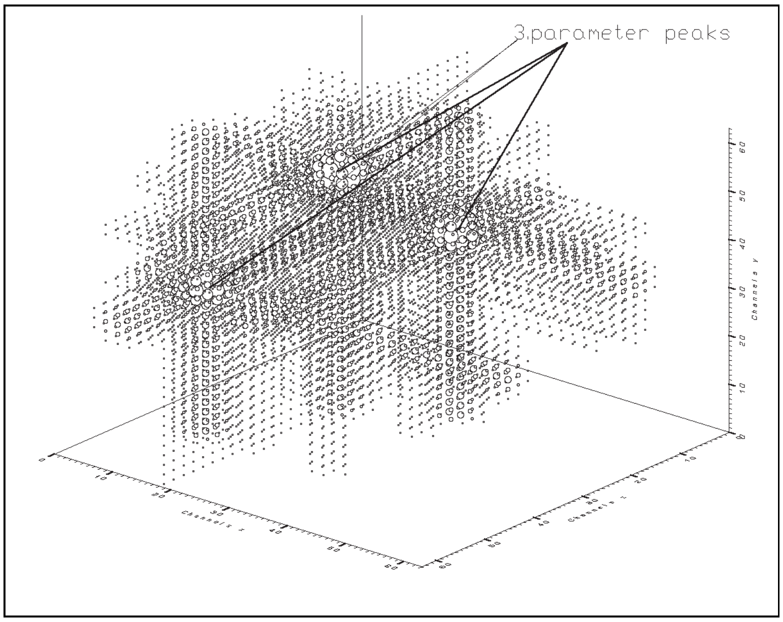

Figure 14: Synthetic three-dimensional spectrum

exactly the positions of three-dimensional peaks in the locations where they were generated. In Fig. 15 we can see found peaks without spectrum. Employed presentation technique allows to read-out in a simple way the positions of found peaks. Likewise we have used the derived algorithm to search for peaks in the real three-dimensional spectrum (Fig. 16). The found peaks in this spectrum are shown in Fig. 17. Again this example gives evidence that the method is insensitive to crossing of lower-fold coincidences.

5 Conclusions

The paper presents the peak searching algorithms for two- and three-dimensional spectra. The algorithm was generalized for m-dimensional spectra as well. The derived algorithms are insensitive to both lower-fold coincidences peak-background and their crossings.

The algorithms of peak searching derived in the paper have been implemented in the multiparameter nuclear data acquisition and processing system [11], [12]. They have been employed to process one-, two- and three-dimensional spectra from experiments in LBL Berkeley, which are realized in collaboration with Vanderbilt University, JINR Dubna, Idaho National Engineering Laboratory and Oak Ridge National Laboratory.

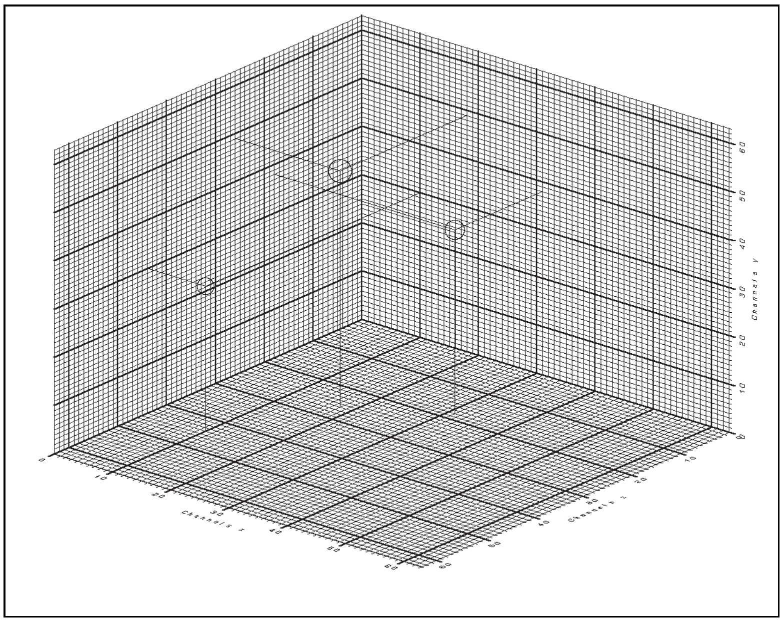

Figure 15: Found peaks in three-dimensional spectrum

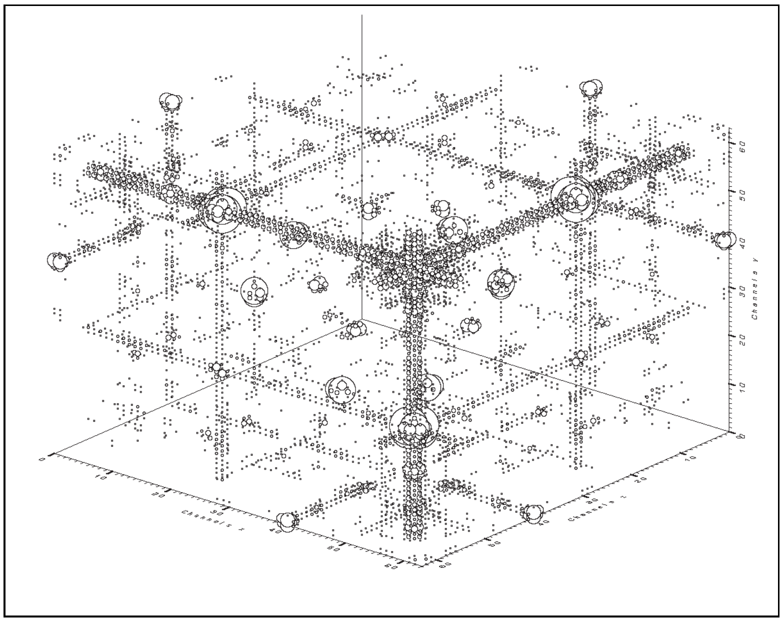

Figure 16: Real three-dimensional spectrum

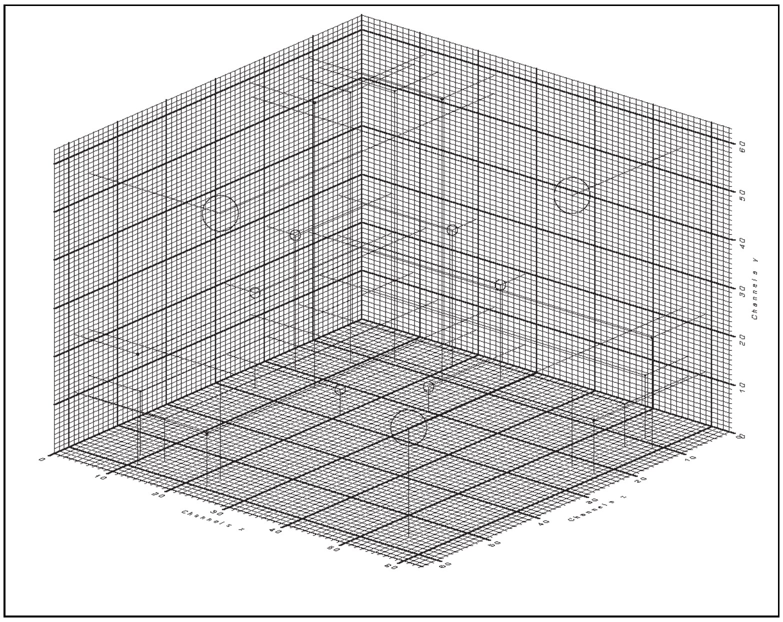

Figure 17: Found peaks in three-dimensional spectrum from Fig. 16

Acknowledgments
The work was partially supported by the Grant Agency of Slovak Republic through contract GAV 2/5121/98. The authors would like to thank the Gammasphere collaboration, J. H. Hamilton, J. O. Rasmussen, G. M. Ter-Akopian and A. V. Daniel for the help in data preparation and valuable discussions.

References

[1] F. A. Beck, Prog. Part. Nucl. Phys., 28, (1992) 443.

[2] M. A. Delaplanque, R. M. Diamond (Eds.) GAMMASPHERE a National Gamma-Ray Facility, a proposal, March 1988 .

[3] C. Ross-Alvarez, Nucl. Phys. News Europe 3, (1993) 10.

[4] M. A. Mariscotti, Nucl. Instr. and Meth.. 50, (1967) 309.

[5] J. T. Routti and S. G. Prussin, Nucl. Instr. and Meth., 72 (1969) 125.

[6] Ö. Giftcioglu, Nucl. Instr. and Meth. 174, (1980) 209.

[7] I. A. Slavič and S. P. Bigulac, Nucl. Instr. and Meth., 84, (1970) 261.

[8] G. W. Phillips, Nucl. Inst. and Meth. 153, (1978) 449.

[9] Z. K. Silagadze, Nucl. Instr. and Meth. A 376 (1996) 451.

[10] J. Krištiak, K. Krištiaková, O. Šauša, P. Bandžuch, J. Bartoš, J. de Phys., 3, (1993) 265.

[11] M. Morháč, I. Turzo, J. Krištiak,, IEEE Trans. on Nucl. Sci. 42, (1995) 1.

[12] M. Morháč, J. Kliman, V. Matoušek, I. Turzo, Nucl. Instr. and Meth. A 389 (1997) 89.